



HAL
open science

Improved bend over sheave durability of HMPE ropes for deep sea handling

Peter Davies, Nicolas Lacotte, Maël Arhant, Damien Durville, Abderrahim Belkhabbaz, Michel François, Fabien Khouri, Kara Konate, Stephen Mills, Jean-Robert Philippe, et al.

► To cite this version:

Peter Davies, Nicolas Lacotte, Maël Arhant, Damien Durville, Abderrahim Belkhabbaz, et al.. Improved bend over sheave durability of HMPE ropes for deep sea handling. 37th International Conference on Ocean, Offshore and Arctic Engineering, Jun 2018, Madrid, Spain. 10.1115/OMAE2018-77530 . hal-02458734

HAL Id: hal-02458734

<https://centralesupelec.hal.science/hal-02458734>

Submitted on 16 Oct 2020

HAL is a multi-disciplinary open access archive for the deposit and dissemination of scientific research documents, whether they are published or not. The documents may come from teaching and research institutions in France or abroad, or from public or private research centers.

L'archive ouverte pluridisciplinaire **HAL**, est destinée au dépôt et à la diffusion de documents scientifiques de niveau recherche, publiés ou non, émanant des établissements d'enseignement et de recherche français ou étrangers, des laboratoires publics ou privés.



Distributed under a Creative Commons Attribution 4.0 International License

IMPROVED BEND OVER SHEAVE DURABILITY OF HMPE ROPES FOR DEEP SEA HANDLING

Peter Davies, Nicolas Lacotte, Mael Arhant
IFREMER
Plouzané, France

Damien Durville, Abderrahim Belkhabbaz
Centrale-Supelec
Gif-sur-Yvette, France

**Michel François,
Fabien Khouri**
Bureau Veritas
La Défense, France

**Kara Konate,
Stephen Mills**
IMECA-REEL
La Rochelle, France

**Jean-Robert Philippe,
Christophe DeFrance**
CyXplus
Montbonnot, France

Paul Smeets
DSM Dyneema
Geleen, Netherlands

**Dennis Sherman,
Kurt Newboles**
Samson Ropes
Ferndale, USA

Alain Ledoux
TOTAL S.A.
La Défense, France

**Nicolas Chazot,
Sebastien Saillard**
Saipem
Saint Quentin, France

**Ramesh Kante,
David Cannell**
TechnipFMC
Aberdeen, UK

**Patrick Chevallier,
Olivier Lodeho**
Subsea7
Paris, France

ABSTRACT

The use of synthetic fiber ropes for subsea installation is extending, as the offshore industry explores deeper waters, but there are few data available to evaluate the lifetime of these materials. In a previous OMAE presentation the authors described results from the first phase (2010-2013) of a JIP aiming to understand the mechanisms controlling the long term behavior of HMPE fibre ropes [1]. This presentation will describe the results from the second phase of this study (2014-2018) in which predictive models have been developed and applied to a range of improved braided rope materials. Two modeling approaches will be discussed, an empirical method based on residual strength after cycling, and a numerical approach using finite element software specifically adapted to fibre materials [2]. An extensive test program, which has generated a database of CBOS (cyclic bend over sheave) results for various grades of HMPE and different constructions, will be described. Comparisons have been made with steel wire handling lines in order to quantify the benefits of fibre ropes for these deepwater applications.

INTRODUCTION

Synthetic fibre ropes are finding increasing marine applications where steel wire ropes are too heavy. Polyester fibre mooring lines for floating offshore platforms are now well accepted [3,4] and fibre ropes for station-keeping of renewable marine energy installations is also attracting considerable interest [5]. These applications are based on tension loading, both quasi-static and dynamic, but do not require resistance to bending. The deep sea handling applications are different as ropes are lowered by winches and usually pass over several sheaves before entering the water. As a result it is their bending over sheave resistance which defines their useful lifetime. The low weight in water of fiber ropes is a key advantage with respect to steel, and the possibility to repair by cutting and splicing is also beneficial. However, it is essential to ensure that their bend over sheave performance is adequate and this is the subject of the present work.

CITEPH JIP2 PROGRAMME

The work presented here was performed as a JIP within the CITEPH framework [6]. This is a French program to facilitate access to private funding of innovative R&D projects in Oil & Gas and related energy industries.

MATERIALS

The study focused on 12 strand braided ropes produced from Dyneema® SK78 and DM20 fibres. Three rope variants of the Dyneema® SK78 fibres were studied, one 18mm diameter, one 24mm and one 24mm diameter with a 12 x 3 construction. The 18mm ropes were studied to investigate the influence of fibre types and finishes. The 24mm ropes were chosen to examine size effects and the effect of construction on performance. The reference material is a braid with a DPX rope design from Samson Ropes, who also supplied improved braids based on Dyneema® SK78 XBO and Dyneema® .DM20 XBO fibers for optimized CBOS performance. Two variants of the Dyneema® DM20 fibre ropes were studied, the standard grade and the one with XBO technology. Figure 1 shows the six types of specimen received for testing. The DPX was developed to improve friction on traction drums, whether it is a grooved drum or independently driven sheaves, while the Dyneema® XBO technology was developed to improve CBOS performance.



Figure 1. Samples supplied for testing.

TEST FACILITIES

The tests presented here were of two types, tensile loading and cyclic bend over sheave (CBOS), both performed up to failure.

First, break tests were performed on the six materials. Three eight-meter long samples of each, with spliced eyes at each end, were tested to break on a 100 Ton capacity test frame, Figure 2. Samples were cycled five times to 50% of nominal minimum break load to bed them in before a ramp to failure. A non-contact extensometry system, based on two digital cameras, was used to measure strains in the central part of the sample up to failure, away from the splices.

The CBOS tests were performed on a specially designed 3-hydraulic piston test frame at IFREMER; the central piston allows a constant load to be maintained on a sample, while the

two outer pistons apply a back and forth displacement over the sheave, Figure 3 [1]. The loads and displacements of all 3 pistons are recorded continuously throughout the tests. Loads were in the range from 10 to 50% of tensile break load. For initial tests an IR camera was also employed to check rope surface temperature variations.

The CBOS tests were all performed with continuous wetting. The D/d (Sheave/Rope diameter) ratio was 20, cycling period was 20 seconds (for two bends-unbends), displacement was 350mm for 18mm diameter, and 480mm for 24mm diameter ropes. Displacements were chosen to ensure that the central section of the rope was subjected to a complete bend-unbend cycle.



Figure 2. Sample on test frame.



Figure 3a. CBOS test machine



Figure 3b. Sample on sheave during CBOS test.
N.B. Braided ring on top of sheave is reference for InfraRed camera temperature measurements.

BREAK TEST RESULTS

Figure 4 shows examples of plots from two straight pull tensile break tests, on ropes of two diameters, normalized with respect to their break loads.

The smaller rope shows slightly higher permanent bedding-in strain on first loading, which may be induced by storage or handling, but beyond this the behaviors are very similar. The load-strain response of bedded-in ropes is quite linear. Failures occurred in the central rope sections.

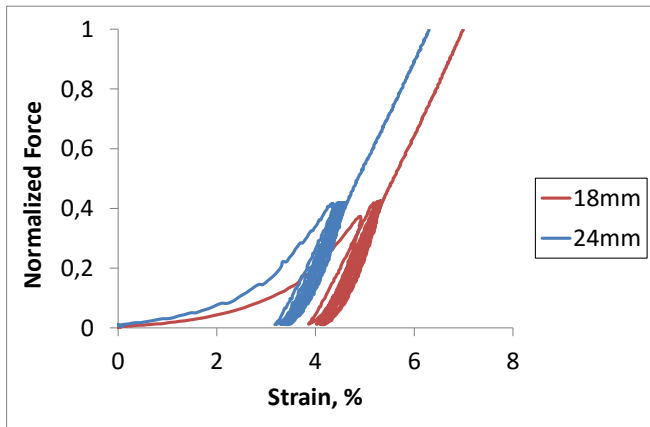


Figure 4. Break test plots for Dyneema® SK78-DPX 12x1 braided ropes of two diameters.

CBOS TEST RESULTS

A large number of CBOS tests to failure were performed, in order to obtain the applied load versus cycle to failure (T-N_f) plot, Figure 5. This shows very clearly the influence of the XBO technology, which increases the rope lifetime by a factor of 3 to

10. Ropes based on Dyneema® DM20-XBO provide the longest lifetimes.

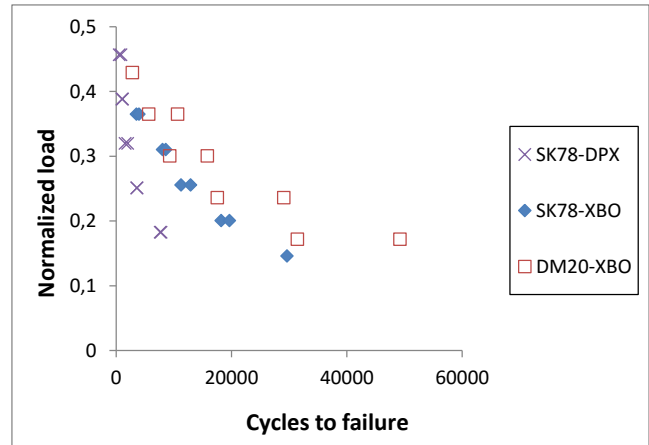


Figure 5. CBOS T-N_f plots, 18mm braided ropes. Load normalized by tensile break load

Then tests were interrupted at different proportions of the lifetime in order to determine how the residual strength changed during cycling. The residual strength was measured by cycling on the sheave under increasing load from the CBOS test value up to failure. This testing procedure has been shown to be considerably less conservative than measuring residual strength, with a tensile ramp to failure, and it is also more relevant to the handling application [1]. Figure 6 provides an example of residual cycling on sheave results for interrupted tests after cycling for different numbers of cycles at a load of 18% of the tensile break strength. Samples were kept in tension at all times. All samples failed in the central zone of the rope which had been worked on the sheave.

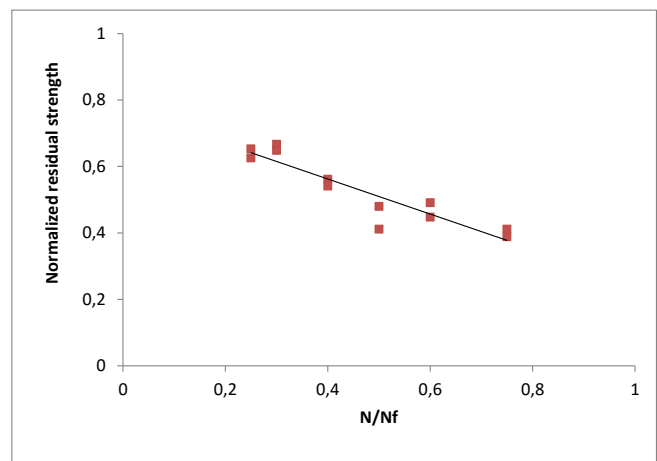


Figure 6. Residual strengths after interrupted cycling for different periods at 18% of tensile break load, SK78-DPX 18mm. Strengths normalized by tensile break load.

There is an approximately linear drop in residual strength with cycling.

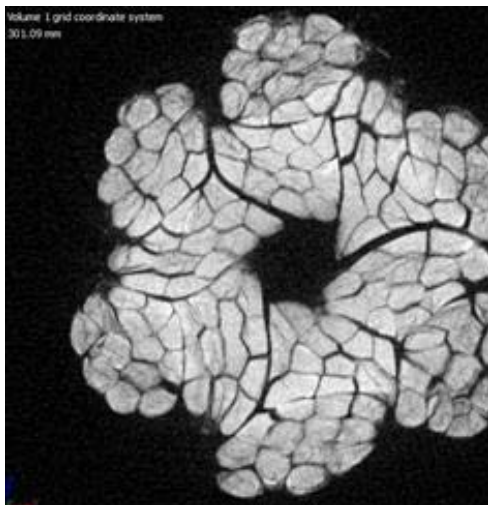
X-RAY TOMOGRAPHY

After failure it is not easy to determine the sequence of events leading to final break. In order to examine the damage development some tests were interrupted after different numbers of cycles. The samples were then cut to remove the most heavily loaded zones, which were examined in an X-ray tomograph at CyXplus, Figure 7.

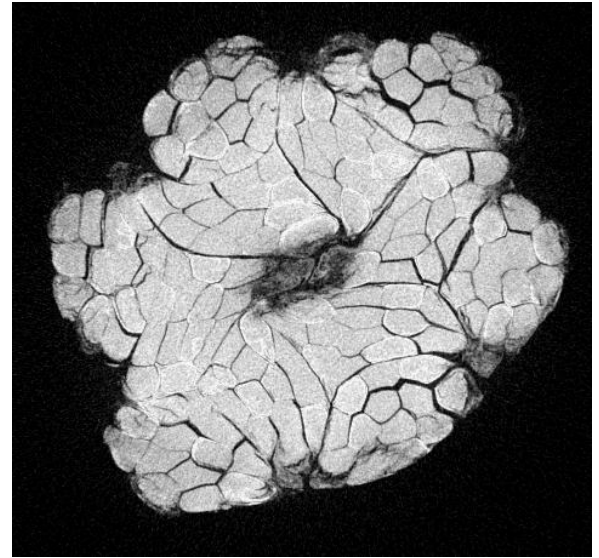


Figure 7. Rope sample in tomograph.

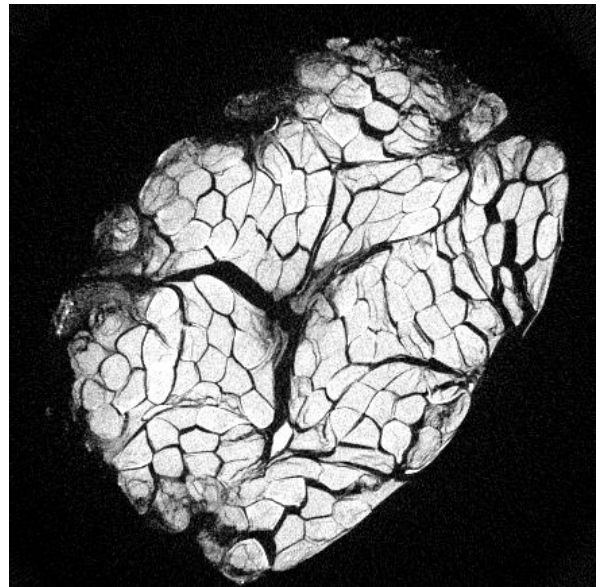
This allows 3-D images of the interior of the rope to be reconstructed. Figure 8 shows examples of the information provided by this technique



(a)



(b)



(c)

Figure 8. Images of 24mm 12x1 rope samples after interrupted CBOS test to 90% of N_f .

- a) From zone with no bending (only tension)
- b) From single bend zone.
- c) From double bend zone
- d)

These images show the compaction of the rope as it takes the form of the sheave (bottom right of images (b) and (c)), and the development of both external and internal damage as failure approaches.

EMPIRICAL MODEL

In order to apply the data generated in the project to practical applications an empirical analysis has been developed by Bureau Veritas [7].

First, the Tension-Nf data are fitted to trend lines by linear regression (least square fit) of $\log N_f$ versus $\log T$, following the classical relation:

$$\log N_f = \log K - m \log T \quad \text{i.e. } N_f \cdot T^m = K$$

in which the (inverse) slope parameter m is found to be in the range of 2.5 to 3.

However, it should be noted that this classical T-N_f endurance curve cannot be used to predict rope lifetime under the effect of varying tension, using a Miner sum, as has been observed from results of the two-load tests described below.

Then the residual strength while cycling data are analysed.

As observed above (figure 6), the strength decay under cycling at a given tension is approximately proportional to the applied number of cycles N (or N/N_f in figure 6). However the rate of strength loss dR_s/dN for different tensions is found to be about proportional to T^b , with b around 1.6, clearly lower than m : this rate is thus not proportional to T^m , i.e. $1/N_f$.

The model proposed, based on the above, can be written as:

$$R_s(N, T) = R_2 - Q \cdot N$$

with:

- Q the rate of strength loss, $Q = a T^b$,
- R_2 the value at the origin,

The parameters of the model (R_2 , a , b) are obtained by a (non-linear) least square fit, and are rope specific.

The value at the origin R_2 is in the range of 70% of the new rope breaking strength in straight pull, and as if the initial drop occurred during the first cycle(s). The progressive drop of strength in the early cycling is thus ignored, which is a conservative assumption for the evaluation of R_s in the early lifetime of a rope. This model also does not address the end of life of a rope, when N approaches N_f , as that is not a desired situation in a real system.

The comparison of measured R_s and the predicted values using the empirical model, Figure 9, shows that a good correlation is obtained.

In a real system, the (mean) tension will not be constant, but likely different for each operation. Given the linearity (in N) of the above equation, R_s for several tensions T_i can be written:

$$R_s = R_2 - \sum Q_i \cdot N_i$$

In which N_i are the number of cycles at each tension, and Q_i the corresponding rate of strength loss.

In order to validate this approach, some interrupted two-load tests were performed with residual strength measurements; a good correlation was obtained between the measured and predicted residual strength, Figure 9.

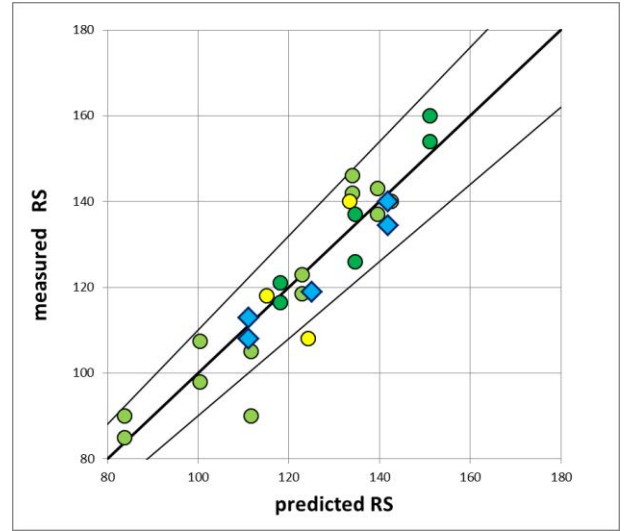


Figure 9. Residual strength model validation: model data for three tensions (circles), two-load tests (blue diamonds), and $\pm 10\%$ interval (lines)

As for classical breaking strength assessment, a design (characteristic) value R_d of the residual strength may be evaluated, taking into account the scatter of data [6]. This can be then rewritten as a T-allowable N_s curve at a given Residual Strength [6], with which the effect of several tensions can be combined by the usual Miner sum.

Then, for a given lifetime under one or several tensions, be it a prediction or monitoring record, a direct assessment of the safety of the rope can be made by comparing the design in-situ residual strength of the rope and the expected maximum dynamic tension in the line.

NUMERICAL MODEL

In parallel with the empirical approach described above, a finite element simulation code [8], specially developed for the modelling of the mechanical behaviour of materials or structures made of entangled filaments, was used. This simulation code, based on an implicit solution scheme, focuses on the modelling of frictional contact interactions between elementary yarns constituting the rope, and between those yarns and the sheave.

The code is used first to determine the a priori unknown initial configuration of the rope, starting from an arbitrary configuration, and letting contact interactions gradually separate interpenetrated yarns until obtaining a configuration at rest [2], satisfying the different multi-stage constructions corresponding to the selected ropes for the current study. The obtained computed configurations for both 12x1 and 12x3 constructions are shown in Figures 10 and 11. Besides geometrical criteria,

these two configurations were validated by comparing their nonlinear responses in tensile tests to experimental data

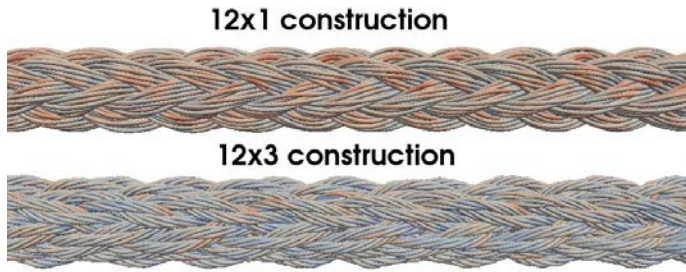


Figure 10. Initial 12x1 and 12x3 braided rope geometry models.

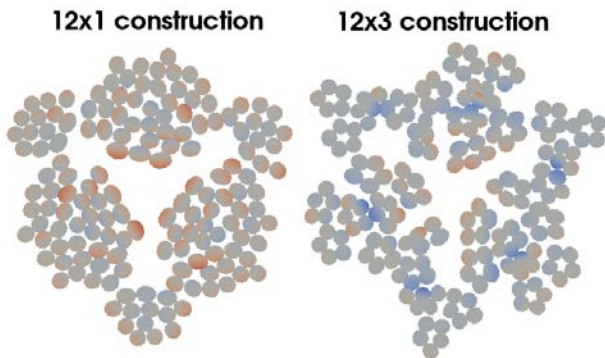


Figure 11. Sections through ropes before bending

Once the initial configuration has been determined, the modelled rope sample is bent on a sheave with a given tension, and then submitted to CBOS. The mechanical loading of individual rope elements can then be examined. This provides a very powerful tool to understand the factors which govern handling rope lifetime.

An example of results, Figure 12, shows a wide range of stresses among yarns. This distribution of stresses results from the geometrical entanglement of yarns within the braided rope, and is increased by frictional interactions induced by relative motions between yarns generated by the change of curvature of the rope at the beginning and at the end of its travel over the sheave. Accurate assessment of stresses at the yarn level allows a better understanding of the influence of mechanisms taking place at the scale of interactions between yarns. Parametric studies were performed to determine the influence of various parameters such as the friction coefficient between yarns and between yarns and sheave, or the D/d ratio.

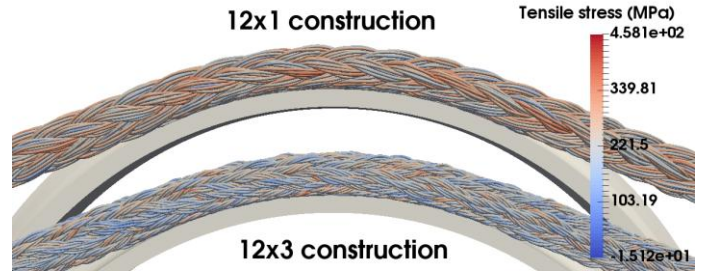


Figure 12. Example of numerical rope model for bending of 24mm diameter ropes with two constructions, 12x1 and 12x3, on a sheave.

Figure 12 reveals the lower stresses in the 12x3 construction, which may explain improved performance (see Figure 15 below).

COMPARISON WITH STEEL WIRE ROPE

In order to establish how these HMPE fibre ropes perform in comparison with the steel wire handling ropes commonly used offshore a small number of additional tests were performed on a 24mm diameter 7x34 construction steel wire rope. Figure 13 shows the rope section.



Figure 13. Steel wire rope cross-section.

Figure 14 shows the rope on the test frame. Two samples were tested wet to failure at each of three load levels.

FUTURE WORK

- Further work is underway within the project to examine scale effects, including thermal modelling.
- Results from tomography are promising but more work is needed. It is essential to develop practical inspection methods for these ropes.

REFERENCES

[1] Davies P, Lacotte N, P, Kibsgaard G, Craig R, Cannell D, François S, Lodeho O, Konate K, Mills S, François M, Defoy A-L, Durville D, Vu D, Gilmore J, Sherman D, Bend over sheave durability of fibre ropes for deep sea handling OMAE2013-11332 OMAE, June 2013, Nantes

[2] Vu TD, Davies P, Durville D, Finite element simulation of the mechanical behaviour of synthetic braided ropes and validation on a tensile test, International Journal of Solids and Structures, Volume 58, April 2015, Pages 106-116

[3] De Pellegrin I, (1999), Manmade fiber ropes in Deepwater Mooring Applications, OTC 10907.

[4] Bugg DL et al, Mad Dog project: Regulatory approval process for the new technology of synthetic (polyester) moorings in the Gulf of Mexico, (2004), OTC16089

[5] Weller SD, Johanning L, Davies P, Banfield SJ, Synthetic mooring ropes for marine renewable energy applications, a review, Renewable Energy, Volume 83, November 2015, Pages 1268–1278

[6] Citeph website, <http://www.citeph.fr/en/>

[7] Davies P, François M, Lacotte N, Vu TD, Durville D, An empirical model to predict the lifetime of braided HMPE handling ropes under cyclic bend over sheave (CBOS) loading, Ocean Engineering, Volume 97, March (2015), Pages 74–81

[8] Durville, D. Contact-friction modeling within elastic beam assemblies: an application to knot tightening. *Computational Mechanics*, 2012, vol. 49, no 6, p. 687-707.

[9] Törnqvist R, Strande M, Cannell D, Gledhill P, Smeets P, Gilmore J, Deployment of Subsea Equipment: Qualification of Large Diameter Fibre Rope for Deepwater Construction Applications, OTC 21588, (2011).